universe

MDPI

Article

Hybrid Isentropic Twin Stars

Juan Pablo Carlomagno [1,2,*], Gustavo A. Contrera [1,2], Ana Gabriela Grunfeld [1,3] and David Blaschke [4,5,6]

[1] Consejo Nacional de Investigaciones Científicas y Técnicas (CONICET), Godoy Cruz, Buenos Aires 2290, Argentina; contrera@fisica.unlp.edu.ar (G.A.C.); ag.grunfeld@conicet.gov.ar (A.G.G.)
[2] Instituto de Física La Plata, Universidad Nacional de La Plata, Consejo Nacional de Investigaciones Científicas y Técnicas (CONICET), Facultad de Ciencias Exactas, Diagonal 113 entre 63 y 64, La Plata 1900, Argentina
[3] Departamento de Física, Comisión Nacional de Energía Atómica, Av. Libertador 8250, Buenos Aires 1429, Argentina
[4] Institute for Theoretical Physics, University of Wroclaw, Max Born Pl. 9, 50-204 Wroclaw, Poland; david.blaschke@uwr.edu.pl
[5] Helmholtz-Zentrum Dresden-Rossendorf (HZDR), Bautzner Landstrasse 400, 01328 Dresden, Germany
[6] Center for Advanced Systems Understanding (CASUS), Untermarkt 20, 02826 Görlitz, Germany
* Correspondence: carlomagno@fisica.unlp.edu.ar

Abstract: We present a study of hybrid neutron stars with color superconducting quark matter cores at a finite temperature that results in sequences of stars with constant entropy per baryon, s/n_B = const. For the quark matter equation of state, we employ a recently developed nonlocal chiral quark model, while nuclear matter is described with a relativistic density functional model of the DD2 class. The phase transition is obtained through a Maxwell construction under isothermal conditions. We find that traversing the mixed phase on a trajectory at low $s/n_B \lesssim 2$ in the phase diagram shows a heating effect, while at larger s/n_B the temperature drops. This behavior may be attributed to the presence of a color superconducting quark matter phase at low temperatures and the melting of the diquark condensate which restores the normal quark matter phase at higher temperatures. While the isentropic hybrid star branch at low $s/n_B \lesssim 2$ is connected to the neutron star branch, it becomes disconnected at higher entropy per baryon so that the "thermal twin" phenomenon is observed. We find that the transition from connected to disconnected hybrid star sequences may be estimated with the Seidov criterion for the difference in energy densities. The radii and masses at the onset of deconfinement exhibit a linear relationship and thus define a critical compactness of the isentropic star configuration for which the transition occurs and which, for large enough $s/n_B \gtrsim 2$ values, is accompanied by instability. The results of this study may be of relevance for uncovering the conditions for the supernova explodability of massive blue supergiant stars using the quark deconfinement mechanism. The accretion-induced deconfinement transition with thermal twin formation may contribute to explaining the origin of eccentric orbits in some binary systems and the origin of isolated millisecond pulsars.

Keywords: hot neutron stars; color superconductivity; thermal twin stars; quark deconfinement

Citation: Carlomagno, J.P.; Contrera, G.A.; Grunfeld, A.G ; Blaschke, D. Hybrid Isentropic Twin Stars. *Universe* **2024**, *10*, 336. https://doi.org/10.3390/universe10090336

Academic Editor: Panos Christakoglou

Received: 23 June 2024
Revised: 13 August 2024
Accepted: 19 August 2024
Published: 23 August 2024

1. Introduction

Exploring the phases of matter under extreme conditions, like those in the early universe or within neutron stars, is a topic that has attracted significant attention in recent decades. We are particularly interested in studying transitions between different phases of strongly interacting matter, like quark–gluon plasma, color superconducting quark matter, and hadronic matter. These transitions have a big impact on astrophysical phenomena like the formation of eccentric binaries and isolated millisecond pulsars (MSPs), binary neutron star mergers, and they even trigger supernova explosions of massive blue supergiant stars [1]. In our recent study [2], we employed a nonlocal quark model [3] that describes these transitions and extended it to the case of finite temperature, also including the effect of neutrino trapping. We were interested in understanding how the transitions

between different phases affect the behavior of hot compact stars, especially when it comes to their formation in the course of supernova explosions and neutron star mergers. The sequence of cold compact stars in the mass–radius diagram behaved "normal" in the sense that it exhibited a branch of pure neutron stars and a branch of hybrid stars with a color superconducting quark matter core which were continuously connected. We observed, however, that at finite temperatures above $T \sim 30$ MeV these branches became disconnected, separated from each other by a branch of unstable configurations[1]. This scenario, in which hybrid stars appear as a separate stable branch of compact stars besides those of neutron stars and white dwarfs, was introduced for cold matter at supranuclear densities by Gerlach [6] in 1968 as that of a third family of compact stars. See also Refs. [7,8] for early applications of the concept to the pion condensate and quark matter phase transitions in neutron stars. The existence of a third family necessarily entails that there exists a common range of masses for stars of the second and third families. For stars exhibiting different radii but the same mass, Glendenning and Kettner introduced the term "twin stars" [9]. Numerous examples for a hybrid equation of state (EOS) that posses mass twins were found immediately after that [10,11], but they did not fulfill the 2 $M_\odot$ mass constraint for pulsars. Twin stars with masses of 2 $M_\odot$ were constructed only after 2013 [4,12,13] (see Ref. [14] for a recent overview on the topic). Let us return to the case of our hybrid star EOS [2], where the twin star phenomenon is found only at finite temperatures but not at $T = 0$. We refer to this siutuation as "thermal twins"—a term that was coined, to the best of our knowledge, in the work of Hempel et al. [15].

Understanding thermal twins better might help solve the puzzle of massive supernova explodability. We want to give a line of argument on how thermal twins and supernova explodability could be related. A recent systematic study of massive supernova explosions [16] within the quark deconfinement mechanism [17] showed that for a successful explosion leaving a stable protoneutron star (PNS) behind, it is important that the PNS undergoes the deconfinement phase transition before the maximum mass for gravitational instability is reached by postbounce mass accretion. While the postbounce mass accretion rate depends on the composition (metallicity) of the progenitor star, the time until the onset of deconfinement in the PNS depends on the hybrid EOS, i.e., the structure of the QCD phase diagram. A normal quark matter EOS results in a lowering of the onset (energy) density of deconfinement with increasing temperature. A lower onset density can be reached faster in the PNS evolution during supernova collapse. A lower energy density at the onset of deconfinement is also beneficial for the appearance of twin stars because of the Seidov criterion for gravitational instability [18]. Elucidating the validity of the Seidov criterion as a condition for the appearance of thermal twin stars is one of the main goals of our work. Another important aspect concerns the character of the deconfinement transition that depends on the slope of the constant entropy per baryon curve in the mixed phase. For $(\partial T/\partial n_B)|_{s/n_B=const} < 0$, the transition is called "entropic" or enthalpic" [15] (see also [19,20]). Up to now, successful supernova explosions with the quark deconfinement mechanism were obtained for a transition to normal quark matter (NQM), which has an entropic character [17,21]. Simulations with a transition to color superconducting quark matter (which is enthalpic [22,23]) have not led to successful explosions [24]. Basically, this is because, at low temperatures relevant for supernovae, the onset density for deconfinement increases with increasing temperature so that the deconfinement transition is not reached in the simulation before the collapse to a black hole sets in.

In the present work, we explore a typical hybrid EOS that results from a Maxwell construction between a hadronic matter (HM) and a quark matter (QM) model that describes a color superconducting (2SC) phase at low temperatures which goes over to the NQM phase at high temperatures. We consider trajectories of constant entropy per baryon in the QCD phase diagram and investigate whether the appearance of thermal twins at increasing temperatures can be associated with an enthalpic-to-entropic character change of the deconfinement transition. We check the applicability of the Seidov criterion as an indicator for the appearance of twin stars in the present case of isentropic hybrid stars.

Therefore, with the present study, we hope to contribute insights into the complex processes happening in the cores of protoneutron stars and during supernova events.

2. Hybrid EOS

To achieve our goals, we used a two-phase model framework to study how matter transitions between hadronic and quark phases in compact stellar environments as presented in Ref. [2]. The hadronic equation is described by a density-dependent relativistic mean-field theory which includes meson–exchange interactions within the "DD2" parametrization [25]. To describe the transition between these phases, we consider a Maxwell construction, which ensures that pressure and Gibbs free energy remain balanced during the transition. Concerning the leptons, our analysis exclusively considered electrons within the system that were incorporated into our model as a free relativistic Fermi gas. We assumed that neutrinos were not trapped in the system. For quark matter, we applied a nonlocal instantaneous NJL-type model, incorporating color superconductivity and local vector repulsive interactions [3]. Nonlocality was introduced in the quark currents through a Gaussian form factor in three-dimensional (3D) momentum space, with the exception of the vector channel. To determine the input parameters for the quark matter model, we first fitted the momentum dependence of the quark mass function from lattice QCD (LQCD) in the Coulomb gauge, obtaining a value for the effective range parameter. Subsequently, we fixed the values of the scalar coupling and the current quark mass based on low-energy phenomenology. A significant advantage of the 3D form factor used in this work is that it allows for analytical Matsubara summations. By combining approaches for both QM and hadrons to build the hybrid EOS, we aim to analyze the impact of the quark–hadron phase transition in (proto)neutron stars, as well as in simulations of supernova explosions and neutron star mergers. We are particularly interested in studying the appearance of thermal twins. We introduce below the QM and hadronic EOS that were used in the present study. This model incorporates a density-dependent bag pressure, and its free parameters were selected to accurately reflect current astrophysical constraints. Details of both models can be found in Refs. [2,3].

2.1. QM EOS

For building the QM EOS, we considered a nonlocal version of the Nambu–Jona-Lasinio model, with a form factor that depends on the three momentum (3DNJL), following Ref. [3]. We considered diquark interactions as well as vector-repulsive interactions. Our earlier findings at zero temperature suggest that incorporating a bag pressure into the quark matter (QM) equation of state (EOS) is necessary to meet modern observational constraints. Additionally, a bag pressure that depends on the baryon chemical potential μ_B is crucial to simultaneously satisfy both radius constraints: $R_{2.0}$ for high-mass neutron stars (NSs) as observed by NICER for PSR J0740+6620, and $R_{1.4}$ for typical-mass NSs based on the tidal deformability from the gravitational wave event GW170817. So, we included a μ_B-dependent bag pressure as follows

$$B(\mu_B) = B_0\, f_<(\mu_B) \tag{1}$$

with

$$f_<(\mu_B) = \frac{1}{2}\left[1 - \tanh\left(\frac{\mu_B - \mu_<}{\Gamma_<}\right)\right], \tag{2}$$

where we considered that $\mu_< = 895$ MeV, $\Gamma_< = 180$ MeV, and $B_0 = 35$ MeV/fm^3. The μ_B-dependent bag pressure affects the value of $n_B = \partial P/\partial \mu_B$. Then, the energy density can be written as follows:

$$\varepsilon = -P^* + T\, s + G^* \tag{3}$$

where $s = -\partial\Omega/\partial T$ and, G^*, the Gibbs free energy, reads

$$G^* = \mu_B\, n_B^* + \mu_l\, n_l + \mu_Q\, n_Q, \tag{4}$$

with $n_B^* = n_B - \partial B(\mu)/\partial \mu_B$ and $P^* = P - B(\mu)$ (the subscripts Q and l stand for quarks and leptons, respectively). The pressure P can be found in [2]. By imposing electric charge neutrality, the last term of Equation (4) is zero; then, G^* can be written as

$$G^* = n_B^* \, \mu_B + n_e \, \mu_e \tag{5}$$

where $n_B = (1/3)(n_u + n_d)$ with $n_f = \sum_c n_{fc}$ and the chemical potentials μ_f are defined in Ref. [3].

2.2. Hadronic EOS

The interactions between baryons in the hadronic phase of nuclear matter are modeled using the density-dependent relativistic mean-field (DDRMF) theory. As mentioned above, details of the model can be found in Ref. [3]. The baryonic pressure reads

$$\begin{aligned} P_B &= \sum_B \frac{\gamma_B}{3} \int \frac{d^3p}{(2\pi)^3} \frac{p^2}{E_B^*} [f_{B-}(p) + f_{B+}(p)] \\ &- \frac{1}{2} m_\sigma^2 \bar{\sigma}^2 + \frac{1}{2} m_\omega^2 \bar{\omega}^2 + \frac{1}{2} m_\rho^2 \bar{\rho}^2 + n\widetilde{R}, \end{aligned} \tag{6}$$

where the electron pressure is given by

$$P_e = \frac{2}{3} \int \frac{d^3p}{(2\pi)^3} \frac{p^2}{E_e} [f_{e-}(p) + f_{e+}(p)] \, , \tag{7}$$

and $f_{B,e\mp}(p)$ are the corresponding Fermi–Dirac distribution functions for electrons and positrons, respectively. Finally, the energy density, ε, is determined by the Gibbs relation:

$$\varepsilon = -P + TS + \sum_j \mu_j \, n_j \, , \tag{8}$$

where $P = P_B + P_e$, $S = \partial P/\partial T$, and $n_j = \partial P/\partial \mu_j$, where j stands for all the particle species of this phase, including electrons. We also added a neutron star crust using the Baym–Pethick–Sutherland (BPS) model [26] to consider the hadronic EOS at densities below the nuclear saturation density.

3. Results for the Hybrid EOS

Before presenting our results for the hybrid EOS, we show in Figure 1 the phase diagram of the nonlocal chiral quark model in the plane of temperature T and baryon chemical potential μ_B. Four regions are shown, which correspond to the chiral symmetry breaking (χSB), normal quark matter (NQM) where the system remains in an asymptotically free phase, and two-flavor color superconducting (2SC) phases as well as a coexistence (COEX) region of 2SC and χSB phases. We considered the same set of parameters as in [3] for the QM EOS. The dashed–double dotted line corresponds to the chiral crossover transition, corresponding to the peak of the chiral susceptibility (as defined in Ref. [3]), and the dashed–dotted line corresponds to a second-order phase transition to the 2SC phase, where the color symmetry is broken. In the normal quark matter phase (NQM), chiral symmetry is restored (partially restored if current quark masses are finite). We also display different solid lines with fixed entropy per baryon number density (s/n_B).

From now on, we will begin the description of the hybrid EOS. In Figure 2, we display the pressure as a function of the baryon chemical potential for both the QM and the HM EOS across various temperatures. The intersections are highlighted with dots and correspond to the Maxwell construction of first-order phase transitions for different isotherms. We observe that as the temperature increases the crossing shifts to lower baryon chemical potentials. In Figure 3, we present the $T - \mu_B - P$ transition points that result from these Maxwell constructions, along with their corresponding two-dimensional projections. The

$P - \mu_B$ projection corresponds to the one presented in Figure 2, while the $T - \mu_B$ projection will be discussed further in Figure 4.

In Figure 4, we present the $T - \mu_B$ phase diagram. The isothermal hadron-to-quark-matter phase transition is shown as a black dotted line, and the colored curves correspond to different fixed values of s/n_B. The dashed–double dotted black line represents the chiral crossover transition calculated at constant T. The dashed–dotted black curve represents the second-order transition from the 2SC phase to the NQM phase. The solid-colored lines correspond to the QM phase, while the dashed lines represent the HM phase. Note that the lines of constant s/n_B exhibit a small jump between the HM and QM phases. The difference between the HM and QM entropy per baryon is denoted by $\Delta_{s/n_B} = [s/n_B]_{QM} - [s/n_B]_{HM}$.

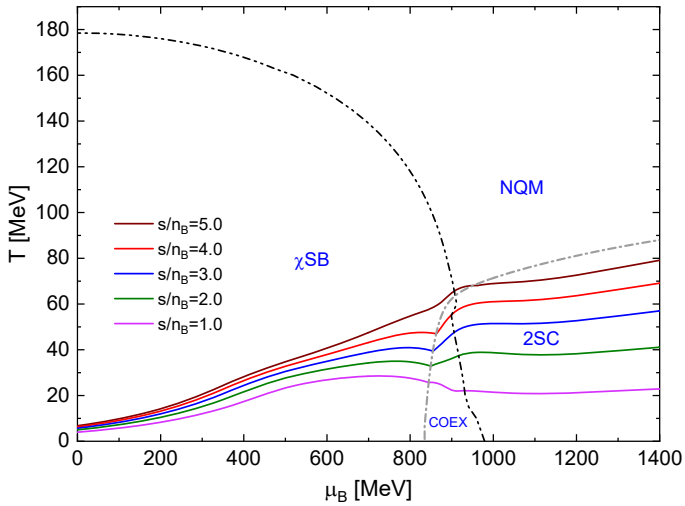

Figure 1. Phase diagram of the nonlocal chiral quark matter model in the $T - \mu_B$ plane. The black dashed–double dotted line corresponds to the chiral crossover transition while the grey dashed–dotted line shows the second-order phase transition to 2SC. The solid-colored lines correspond to points with a constant entropy per baryon ratio s/n_B.

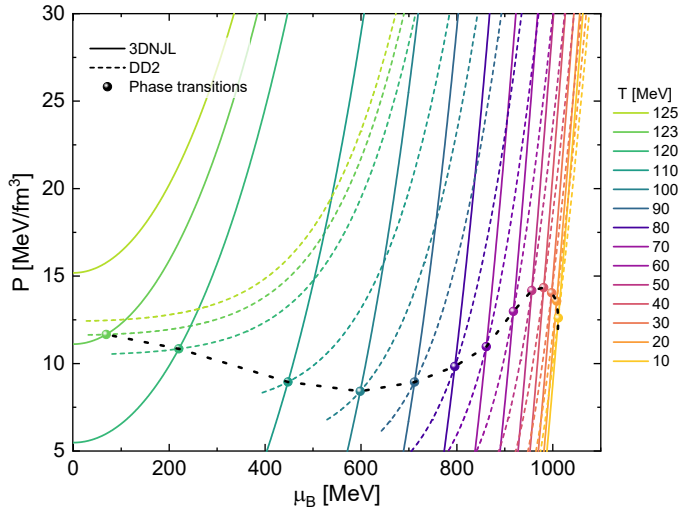

Figure 2. Isotherms of pressure vs. the baryochemical potential for the hadronic DD2 model (dashed lines) and the nonlocal chiral quark model 3DNJL (solid lines). The highlighted crossing points indicate the Maxwell construction of first-order phase transitions.

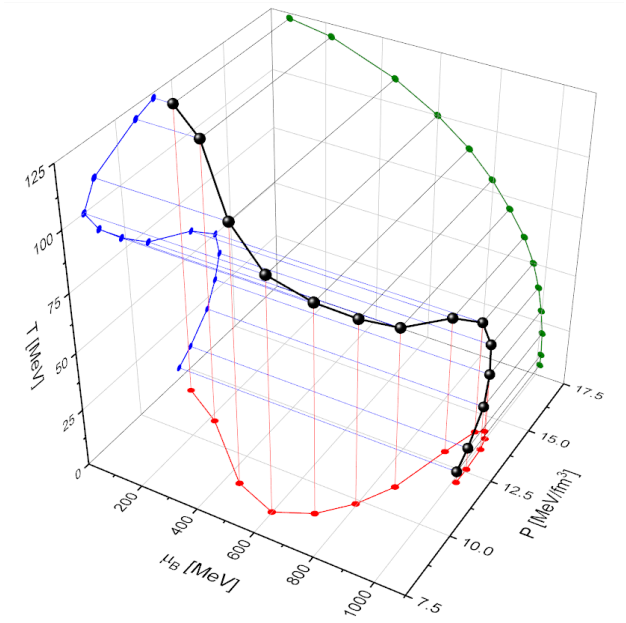

Figure 3. Maxwell transition points in the $T - \mu_B - P$ space (shown as black dots) and the corresponding two-dimensional projections (shown as colored dots).

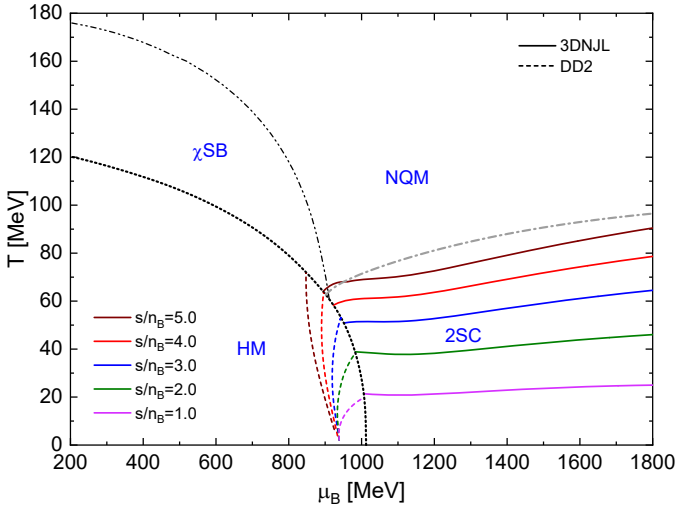

Figure 4. Constant entropy per baryon trajectories for the DD2 hadronic EOS (dashed lines) and for the 3DNJL superconducting quark matter EOS (solid lines) in the QCD phase diagrams in the $T - \mu_B$ plane. The black dashed–double dotted and the grey dashed–dotted lines indicate the corresponding QM phase transitions as in Figure 1.

Up to $s/n_B \approx 2$, the curve of the HM phase remains below its corresponding QM curve at the isothermal phase transition. This corresponds to an enthalpic transition; otherwise, it is considered an entropic one [19,21].

Note that for the special case of $s/n_B = 5$, shown in Figure 4, the corresponding QM line (brown) is not entirely contained in the 2SC phase. This effect will have an impact on the speed of sound c_S^2, as will be shown below.

In Figure 5, we depict the $T - n_B$ phase diagram. We observe a jump in the baryon density during the transition from HM to QM. In this Maxwell-like construction, for a given s/n_B, the phases have different temperatures at the transition. For the phase transition intermediate values, we propose a mixed-phase construction similar to the Glendenning scenario [27]. Once the isothermal phase transition (dotted line in Figure 4) is established, the values of T, μ_B, s, n_B, P, and ε for each phase are the corresponding values for T_c and

μ_c at the intersection between the isothermal transition line and each line with constant s/n_B, while the intermediate values along the phase transition are proposed according to the following relation:

$$Y^{mix} = (1-\chi)\, Y^{HM} + \chi\, Y^{QM}, \quad for\ 0 < \chi < 1 \tag{9}$$

where Y stands for T, mu_B, s, n_B, P, and ε.

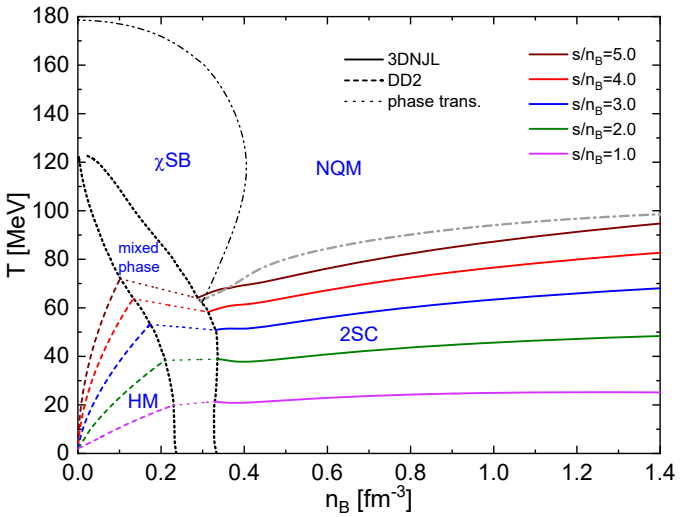

Figure 5. Constant entropy per baryon trajectories for the DD2 hadronic EOS (dashed lines) and for the 3DNJL superconducting quark matter EOS (solid lines) in the QCD phase diagrams in the $T - n_B$ plane. The dotted lines indicate the proposed mixed-phase construction described in the text. The black dashed-double dotted and the grey dashed-dotted lines indicate the corresponding QM phase transitions as in Figure 1.

In Figure 6a, we present P vs. ε for the isentropic curves. It is observed that during the transition from HM to QM phases, there is a plateau where we assume a linear transition. The phase transition is constructed as described before, observing that the isentropic energy densities are different on each side of the transition, while the isentropic pressures are almost the same. Furthermore, it can be noted that the gap in energy density increases with increasing s/n_B as expected. In Figure 6b, we show the isentropic squared speed of sound, corresponding to the slope of Figure 6a. It can be observed that where P vs. ε has a plateau, $c_s^2 = 0$. At large energy densities, the curves do not tend to the conformal limit of $c_s^2 = 1/3$ but, instead, the high-density asymptote falls in the range of c_s^2 = 0.4–0.5.

The peak observed in the brown curve in Figure 6b is associated with the previously mentioned effect where the QM line is not entirely contained within the 2SC phase. This $s/n_B = 5$ QM line, which starts in the χSB phase, crosses to the NQM phase and ultimately ends in the 2SC phase. The peak in c_s^2 is specifically caused by the transition from the NQM to the 2SC phase.

In Figure 7, the isentropic hybrid stellar configurations are shown. The maximum masses of the hybrid stars decrease as s/n_B increases, while the corresponding radii increase. Twin configurations are observed for $s/n_B \geq 2$, where one of the components is hybrid and its counterpart is composed of HM. It is noteworthy that the observed peaks corresponding to the HM–hybrid transitions occur along a straight line (see the dotted line in Figure 7). This line is described by the fit

$$M = C(R - R_0)\,, \tag{10}$$

where $R_0 = 4.20 \pm 0.35$ km is the radius offset and $C = dM_{\rm onset}/dR = 0.0792 \pm 0.0009\ {\rm M}_\odot/{\rm km}$ is the critical compactness of the star for which the deconfinement transition sets in, which for $s/n_B \geq 2$ is accompanied by an instability that entails the formation of a disconnected thermal third-family branch with "thermal twin" stars. In a dynamic setting, such instability is accompanied

by a star quake and burst phenomena. For the results at $T = 0$ that include the modern astrophysical constraints, see Ref. [3].

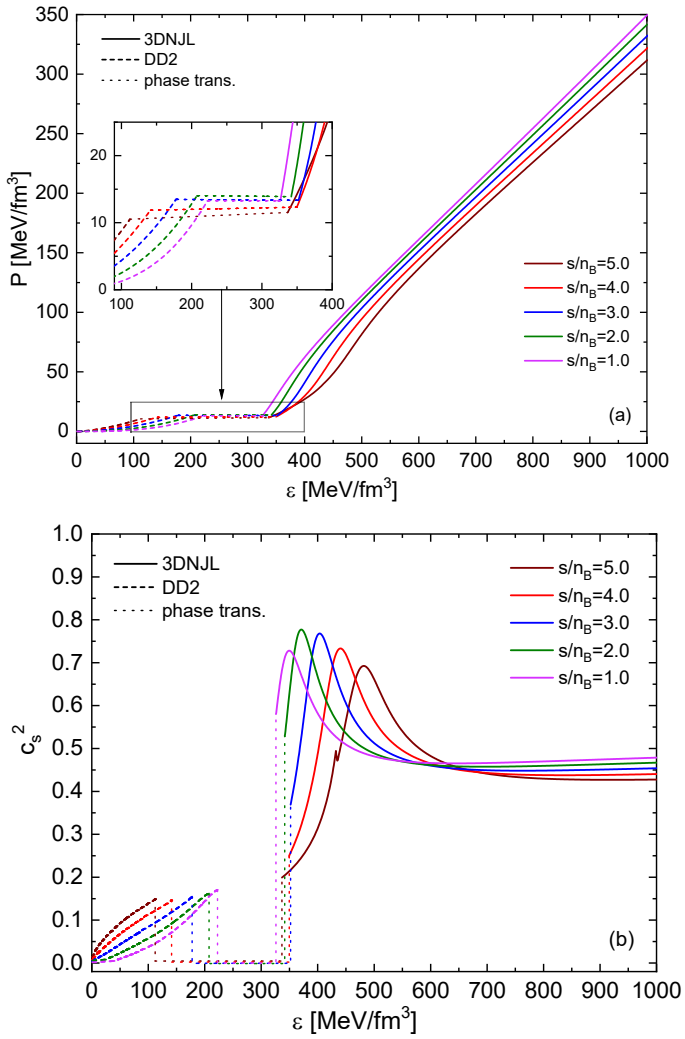

Figure 6. Hybrid EOS (**a**) and squared speed of sound (**b**) as a function of the energy density for different values of entropy per baryon, s/n_B, indicated by different colors.

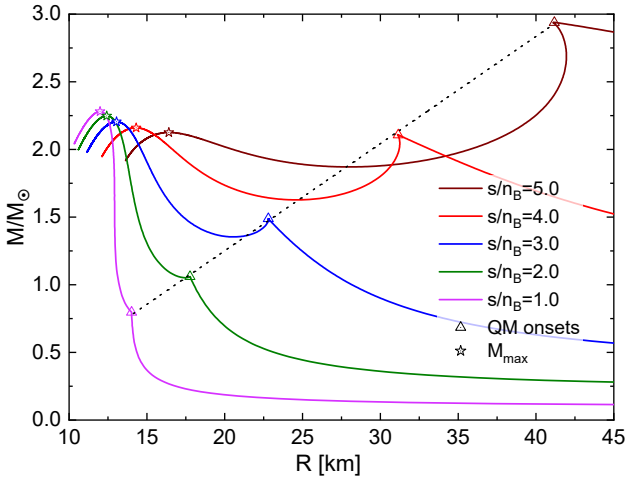

Figure 7. Mass–radius diagram for hot hybrid neutron star sequences with different s/n_B. For $s/n_B \geq 2.0$, one recognizes the occurrence of thermal twin stars. The dotted straight line connects the onset masses for the deconfinement transition.

The onset mass of the deconfinement transition in hot protoneutron star configurations increases systematically with the entropy per baryon (see Figure 8). This behavior can be fitted by the polynomial form

$$\frac{M_{\text{onset}}}{M_\odot} = 0.747 - 0.0373\frac{s}{n_B} + 0.0948\left(\frac{s}{n_B}\right)^2. \tag{11}$$

From Figure 7, it can be observed that the phenomenon of thermal twin star configurations occurs for $s/n_B \geq 2$. At $s/n_B \gtrsim 4$, however, the onset mass of the transition starts exceeding the maximum mass of the hybrid star mass, so that no stable star configuration shall emerge but a collapse to a black hole can be expected. One can read from Figure 8 that the mass range of stable twin stars that can be reached in the accretion-induced transition from a hot protoneutron star lies in the range from 1.0 to 2.2 $M_\odot$ for the corresponding range of entropy per baryon of $s/n_B = 2$–4.

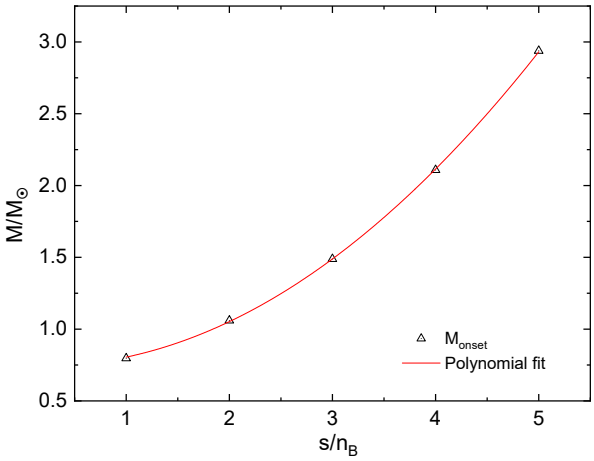

Figure 8. Onset masses for the deconfinement transition as a function of the entropy per baryon (triangle up) s/n_B and a polynomial fit (solid line).

For neutron star phenomenology, it is of interest to estimate the mass defect that corresponds to such a mass twin transition. In order to estimate this quantity for a transition that occurs under the conservation of the baryon number, we calculate both the gravitational mass and the baryon mass as a function of the central energy density by solving the corresponding Tolman–Oppenheimer–Volkoff equations. The result is shown in Figure 9 for selected values of constant entropy per baryon.

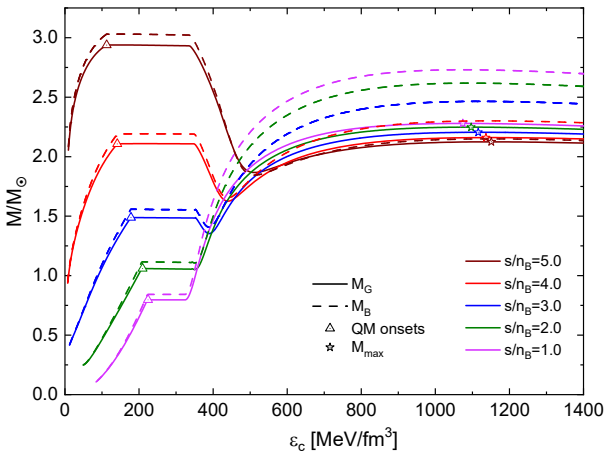

Figure 9. Gravitational mass (solid lines) and baryon mass (dashed lines) versus central energy density for different values of entropy per baryon of the hot hybrid neutron star configurations.

In order to construct the mass defect from these solutions, one zooms into the twin transition mass range and finds the corresponding central energy densities with the identical (critical) baryon mass. Then, one reads off the gravitational masses of these twin configurations and finds the mass defect. See Figures 10–12 for the illustration of this construction in cases where $s/n_B = 4.0, 3.0, 2.0$, respectively.

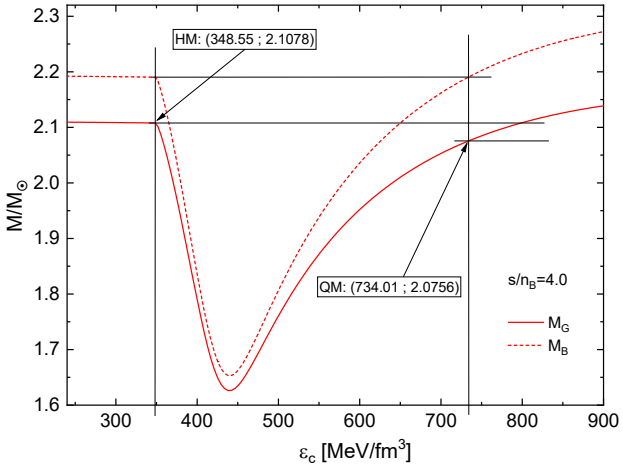

Figure 10. Gravitational mass defect construction for $s/n_B = 4.0$.

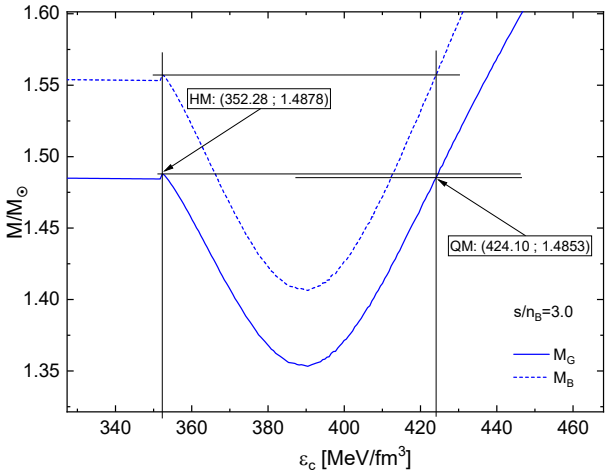

Figure 11. Same as Figure 10 for $s/n_B = 3.0$.

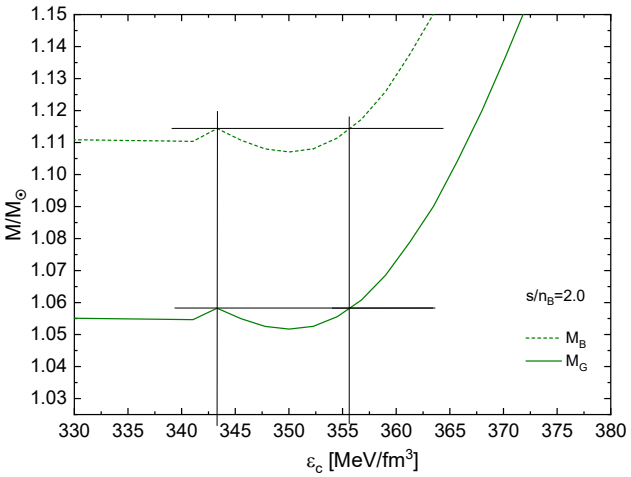

Figure 12. Same as Figure 11 for $s/n_B = 2.0$.

This construction was performed for further representative values of entropy per baryon and the results are summarized in Table 1. Since the transition is considered an isentropic process, the temperature in the star generally has to change. We also display the change in the central temperature in Table 1, defined as $\Delta T(0) = T(0)_{QM} - T(0)_{HM}$, to characterize the type of the deconfinement transition as an entropic process ($\Delta T(0) < 0$) or an enthalpic one ($\Delta T(0) > 0$) (see Refs. [15,19,21] for further details).

Table 1. Characterization of the accretion-induced transition from the second to the third family of compact star configurations under conservation of baryon mass $M_{B,tr}$ for different values of entropy per baryon $s/n_B = 2.0, 2.5, 3.0, 3.5, 4.0$. The second column corresponds to the maximum mass of the stable hybrid stars, $R(M^{\max}_{HYB})$. The gravitational mass defect is $\Delta M = M_{G,HM} - M_{G,QM}$ and whether the difference in central temperatures $\Delta T(0) = T(0)_{QM} - T(0)_{HM}$ in the adiabatic transition is positive (negative) determines its character as enthalpic (entropic) (see [15,21]). Masses are in units of the solar mass $M_\odot$, radii in kilometers, and temperatures in MeV.

s/n_B	$R(M^{\max}_{HYB})$	$M_{B,tr}$	$M_{G,HM}$	$M_{G,QM}$	ΔM	$T(0)_{HM}$	$T(0)_{QM}$	$\Delta T(0)$	Character
2.0	12.41	1.114	1.0582	1.0582	0.0000	38.36	38.87	0.51	enthalpic
2.5	12.61	1.311	1.2490	1.2487	0.0003	46.33	45.57	−0.76	entropic
3.0	13.06	1.557	1.4878	1.4853	0.0025	53.16	50.84	−2.32	entropic
3.5	13.58	1.849	1.7726	1.7621	0.0105	58.89	55.01	−3.88	entropic
4.0	14.29	2.190	2.1078	2.0756	0.0322	63.74	58.28	−5.46	entropic

Coming back to the gravitational mass defect, we display this quantity in Figure 13 as a function of the entropy per baryon. While, for $s/n_B = 2.0 - 2.5$, the mass defect is negligibly small, below one per mille of a solar mass, it amounts to 1–3 percent for $s/n_B = 3.5$–4.0. This nonlinear behavior can be fitted by the functional form of an exponential,

$$\Delta M_G / M_\odot = -0.752 \cdot 10^{-4} + 4.96 \cdot 10^{-6} \times \exp(2.2\, s/n_B)\,. \tag{12}$$

Such values of mass defect in a dynamical accretion-induced deconfinement transition scenario have been found recently to be sufficient to explain the origin of a measurable eccentricity of the orbit in millisecond binaries [28–32].

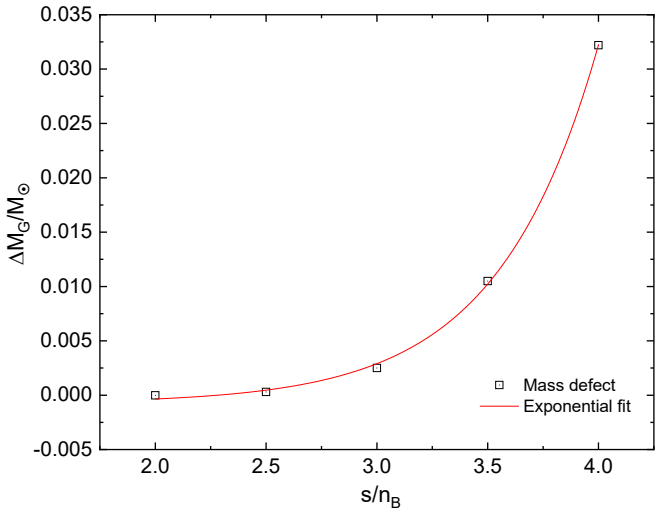

Figure 13. Mass defect vs. s/n_B (open squares) and exponential fit (red solid line).

We note that in Figure 12 it can clearly be seen that before the onset of the instability for $dM/d\varepsilon_c < 0$, there is a small stable branch of hybrid stars, with central densities already exceeding the critical energy densities on the quark matter side of the phase transition. This is not a numerical artifact, but a real physical effect. As has already been found in

Refs. [18,33,34], and discussed more in detail in the framework of the classification of mass–radius curves for hybrid stars by Alford et al. [4], there is a small sequence of stable hybrid stars with a tiny quark matter core that is connected to the hadronic neutron star branch, provided the jump in energy density at the transition is small enough not to fulfill the Seidov criterion [18] for gravitational instability

$$X = 2\Delta\varepsilon - \varepsilon_c^{HM} - 3P_c^{HM} > 0\,. \tag{13}$$

The Seidov criterion (13) for the instability of compact star solutions is a necessary condition for the occurrence of the third family branch of hybrid stars[2].

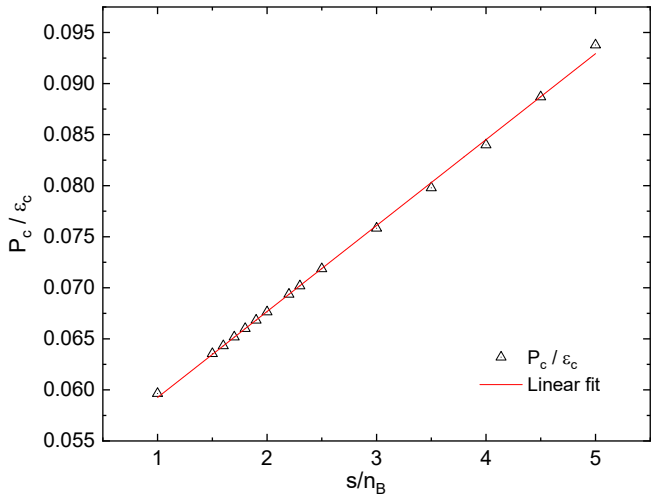

Figure 14. Dimensionless onset critical pressure $P_c^{HM}/\varepsilon_c^{HM}$ vs. s/n_B and a linear fit (red solid line).

We also apply it here (to the best of our knowledge, for the first time) for hot hybrid star configurations as an indicator for the minimal value of the entropy per baryon that is required as a condition for the appearance of the thermal twin star branch

$$X\big|_{(s/n_B)_{\rm crit}} = 0\,. \tag{14}$$

In Figure 15, we show the dependence of X on the entropy per baryon and fit this dependence with a cubic function given by $-51.323 - 57.227(s/n_B) + 59.639(s/n_B)^2 - 6.790(s/n_B)^3$. This allows us to find the zero of this function at $s/n_B = 1.81 \pm 0.04$. In order to test this prediction for the critical entropy per baryon where we expect the onset of the thermal twin behavior, we show in Figures 16 and 17 the mass–radius and mass–central energy density diagrams for the finer interval of $1.5 \leq s/n_B \leq 2.0$, respectively. From the magnified close-ups in the insets, one can confirm that the Seidov criterion (13) works remarkably well in predicting the onset of the thermal mass twin instability. This is not trivial, because the Seidov criterion was derived for the zero temperature case. We conjecture that the successful application of the Seidov criterion is justified in the special case we consider here because the instability occurs in the vicinity of the value $s/n_B \sim 2$, where the deconfinement phase transition is approximately isothermal.

In a subsequent systematic investigation of other hybrid EOSs at finite temperatures, the conjecture for the applicability of the Seidov criterion as an indicator for the onset of the thermal twin instability shall be tested. If the conjecture can be confirmed, this would have significant implications for the phenomenology of protoneutron star evolution during a supernova explosion, as well as for accreting neutron stars in binaries. It would enable statements about dynamical stability based solely on the static properties of the EOS.

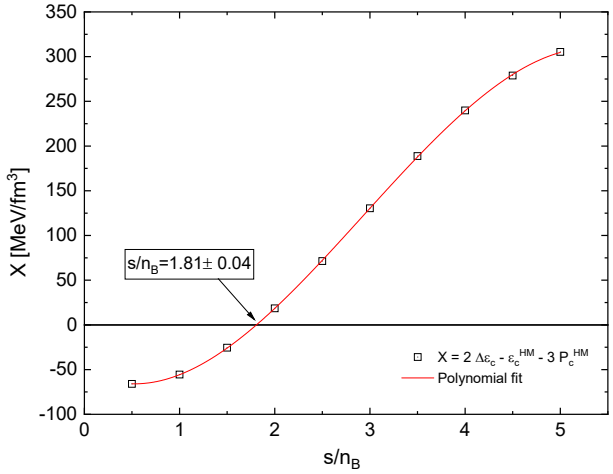

Figure 15. Fulfillment of the Seidov criterion $X > 0$ indicates the gravitational instability that triggers the occurrence of thermal twin star branches (open square symbols). From the polynomial fit (red solid line), we obtain $s/n_B|_{\rm crit} = 1.81 \pm 0.04$. Some additional intermediate QM onset points are included to improve the fit. The inset shows a zoom-in of the region with the onset of the deconfinement transition.

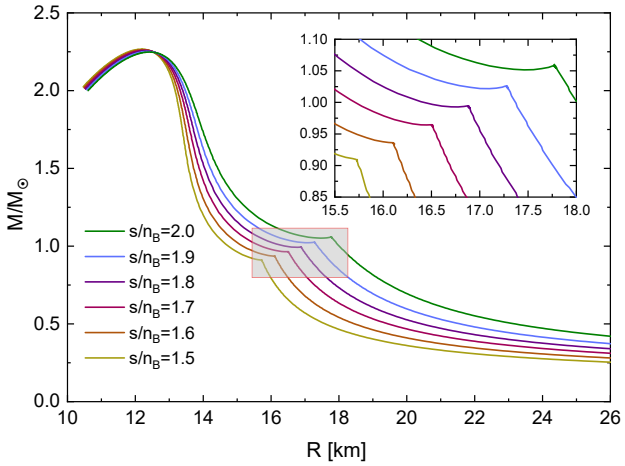

Figure 16. In agreement with the result shown in Figure 15 from the Seidov criterion $X > 0$, this plot shows the onset of twin star configurations after the pointed value of $s/n_B = 1.81$.

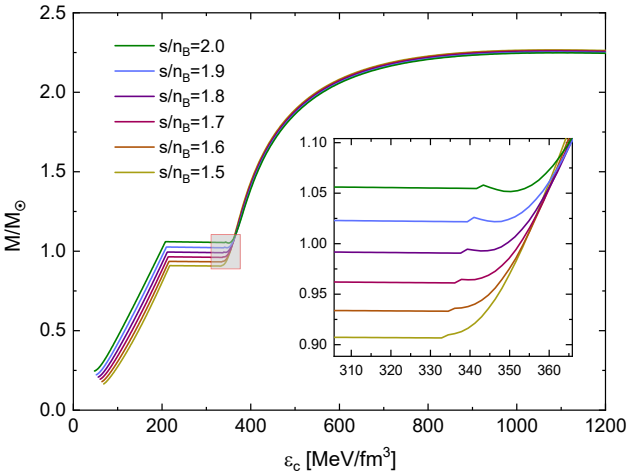

Figure 17. The same as Figure 16 but relating gravitational masses and central energy density.

4. Summary and Conclusions

In this study, we explored hybrid neutron stars featuring color superconducting quark matter cores at finite temperatures, resulting in sequences of stars with constant entropy per baryon. The phase transition was characterized by a Maxwell construction under isothermal conditions. Our analysis reveals that trajectories traversing the mixed phase in the QCD phase diagram exhibit distinct thermal behaviors based on the entropy per baryon (s/n_B). Specifically, we observe at low entropy per baryon ($s/n_B \lesssim 2$) a heating effect that is associated with the enthalpic character of the transition. Conversely, at higher entropy per baryon, the temperature decreases in the mixed phase, thus signaling the entropic character of the transition to the normal quark matter phase. This behavior is attributable to the existence of a color superconducting quark matter phase at low temperatures and the subsequent melting of the diquark condensate, which reinstates the normal quark matter phase at higher temperatures. Interestingly, the isentropic hybrid star branch connected to the neutron star branch at low $s/n_B \lesssim 2$ becomes disconnected at higher entropy per baryon. This disconnection leads to the emergence of the "thermal twin" phenomenon, where two distinct stellar configurations share similar properties. We determined that the transition from connected to disconnected hybrid star sequences can be effectively estimated using the Seidov criterion for the difference in energy densities: $\Delta\varepsilon = \varepsilon_c^{QM} - \varepsilon_c^{HM} \geq [\varepsilon_c^{HM} + 3P_c^{HM}]/2$. Furthermore, we identified a linear relationship between the radii and masses at the onset of deconfinement, which defines a critical compactness for the isentropic star configuration at which the transition occurs. This critical compactness serves as a key parameter in understanding the structural evolution of hybrid neutron stars. For large enough $s/n_B \gtrsim 2$, the transition is accompanied by an instability which may trigger a starquake and burst phenomena. The results of this study may be of relevance for uncovering the conditions for the supernova explodability of massive supergiant stars using the quark deconfinement mechanism. It is planned to use the hybrid EOS with color supercondictivity developed in this work for supernova and neutron star merger simulations.

The present study also provides results for estimating the mass defect that occurs in the thermal twin transition triggered by accretion-induced quark deconfinement for millisecond pulsars in low-mass X-ray binary systems resulting in eccentric orbits or even the formation of isolated millisecond pulsars. Investigations in this direction are prepared for publication [32].

Overall, our study provides valuable insights into the thermal and structural properties of hybrid neutron stars, highlighting the significance of color superconductivity and the role of entropy per baryon in phase transition dynamics. These findings contribute to a deeper understanding of the complex behavior of matter under extreme conditions, as encountered in compact stellar objects.

Author Contributions: Methodology, D.B.; Formal analysis, G.A.C. and D.B.; Investigation, J.P.C., G.A.C., A.G.G. and D.B.; Writing—original draft, A.G.G. and D.B.; Writing—review & editing, J.P.C., G.A.C., A.G.G. and D.B.; Visualization, G.A.C. All authors have read and agreed to the published version of the manuscript.

Funding: A.G.G., G.A.C., and J.P.C. would like to acknowledge CONICET, ANPCyT, and UNLP (Argentina) for financial support under grants No. PIP 2022-2024 GI-11220210100150CO, PICT19-00792, and PICT22-03-00799 and X960, respectively. D.B. was supported by NCN under grant No. 2019/33/B/ST9/03059 (before October 2023) and under grant No. 2021/43/P/ST2/03319 (after April 2024).

Data Availability Statement: The data produced within this project can be obtained from the authors upon reasonable request.

Conflicts of Interest: The authors declare that there is no conflict of interest related to this publication.

Notes

[1] For a full classification of mass–radius relations for hybrid stars, which also includes the possibility that both cases, connected and disconnected hybrid star sequences, are realized simultaneously, see [4,5].

[2] This statement holds provided the dimensionless critical pressure at the onset of the phase transition is small, $P_c^{HM}/\varepsilon_c^{HM} \lesssim 0.1$. Following the analysis of hybrid star classification in Ref. [4], in the interval $0.1 \lesssim P_c^{HM}/\varepsilon_c^{HM} \lesssim 0.15$ a disconnected branch of hybrid stars as a necessary condition for mass twin stars can also occur in the region (B) below the Seidov line, where the condition (13) is not fulfilled. As we show in Figure 14, for the whole range of entropy per baryon values considered in this work $1 \leq s/n_B \leq 5$, the dimensionless critical pressure follows a linear dependence and stays below 0.1.

References

1. Bauswein, A.; Blaschke, D.; Fischer, T. Effects of a strong phase transition on supernova explosions, compact stars and their mergers. *arXiv* **2022**, arXiv:2203.17188. [CrossRef]
2. Carlomagno, J.P.; Contrera, G.A.; Grunfeld, A.G.; Blaschke, D. Thermal twin stars within a hybrid equation of state based on a nonlocal chiral quark model compatible with modern astrophysical observations. *Phys. Rev. D* **2024**, *109*, 043050. [CrossRef]
3. Contrera, G.A.; Blaschke, D.; Carlomagno, J.P.; Grunfeld, A.G.; Liebing, S. Quark-nuclear hybrid equation of state for neutron stars under modern observational constraints. *Phys. Rev. C* **2022**, *105*, 045808. [CrossRef]
4. Alford, M.G.; Han, S.; Prakash, M. Generic conditions for stable hybrid stars. *Phys. Rev. D* **2013**, *88*, 083013. [CrossRef]
5. Alford, M.G.; Han, S. Characteristics of hybrid compact stars with a sharp hadron-quark interface. *Eur. Phys. J. A* **2016**, *52*, 62. [CrossRef]
6. Gerlach, U.H. Equation of State at Supranuclear Densities and the Existence of a Third Family of Superdense Stars. *Phys. Rev.* **1968**, *172*, 1325–1330. [CrossRef]
7. Kampfer, B. On the possibility of stable quark and pion-condensed stars. *J. Phys. A Math. Gen.* **1981**, *14*, L471–L475. [CrossRef]
8. Kämpfer, B. On stabilizing effects of relativity in cold spheric stars with a phase transition in the interior. *Phys. Lett. B* **1981**, *101*, 366–368. [CrossRef]
9. Glendenning, N.K.; Kettner, C. Nonidentical neutron star twins. *Astron. Astrophys.* **2000**, *353*, L9.
10. Schertler, K.; Greiner, C.; Schaffner-Bielich, J.; Thoma, M.H. Quark phases in neutron stars and a 'third family' of compact stars as a signature for phase transitions. *Nucl. Phys. A* **2000**, *677*, 463–490. [CrossRef]
11. Mishustin, I.N.; Hanauske, M.; Bhattacharyya, A.; Satarov, L.M.; Stoecker, H.; Greiner, W. Catastrophic rearrangement of a compact star due to the quark core formation. *Phys. Lett. B* **2003**, *552*, 1–8. [CrossRef]
12. Blaschke, D.; Alvarez-Castillo, D.E.; Benic, S. Mass-radius constraints for compact stars and a critical endpoint. *PoS* **2013**, *CPOD2013*, 063. [CrossRef]
13. Benic, S.; Blaschke, D.; Alvarez-Castillo, D.E.; Fischer, T.; Typel, S. A new quark-hadron hybrid equation of state for astrophysics—I. High-mass twin compact stars. *Astron. Astrophys.* **2015**, *577*, A40. [CrossRef]
14. Christian, J.E. Neutron Star Equations of State with a Phase Transition in a Relativistic Mean Field Approach at Finite Temperatures. Ph.D. Thesis, Goethe University Frankfurt, Frankfurt, Germany, 2023. [CrossRef]
15. Hempel, M.; Heinimann, O.; Yudin, A.; Iosilevskiy, I.; Liebendörfer, M.; Thielemann, F.K. Hot third family of compact stars and the possibility of core-collapse supernova explosions. *Phys. Rev. D* **2016**, *94*, 103001. [CrossRef]
16. Largani, N.K.; Fischer, T.; Bastian, N.U.F. Constraining the Onset Density for the QCD Phase Transition with the Neutrino Signal from Core-collapse Supernovae. *Astrophys. J.* **2024**, *964*, 143. [CrossRef]
17. Fischer, T.; Bastian, N.U.F.; Wu, M.R.; Baklanov, P.; Sorokina, E.; Blinnikov, S.; Typel, S.; Klähn, T.; Blaschke, D.B. Quark deconfinement as a supernova explosion engine for massive blue supergiant stars. *Nature Astron.* **2018**, *2*, 980–986. [CrossRef]
18. Seidov, Z.F. The Stability of a Star with a Phase Change in General Relativity Theory. *Soviet Astron.* **1971**, *15*, 347.
19. Iosilevskiy, I. Entropic and enthalpic phase transitions in high energy density nuclear matter. In *Compact Stars in the QCD Phase Diagram IV*; Blaschke, D.; Fischer, T., Eds.; Unpublished work (code eConf C140926 (2015)), 2015.
20. Yudin, A.V.; Razinkova, T.L.; Nadyozhin, D.K. Model equation of state to investigate the structure and evolution of superdense stars with a phase transition. *Astron. Lett.* **2013**, *39*, 161–170. [CrossRef]
21. Jakobus, P.; Mueller, B.; Heger, A.; Motornenko, A.; Steinheimer, J.; Stoecker, H. The role of the hadron-quark phase transition in core-collapse supernovae. *Mon. Not. R. Astron. Soc.* **2022**, *516*, 2554–2574. [CrossRef]
22. Blaschke, D.B.; Sandin, F.; Skokov, V.V.; Typel, S. Accessibility of Color Superconducting Quark Matter Phases in Heavy-ion Collisions. *Acta Phys. Polon. Supp.* **2010**, *3*, 741–746.
23. Ivanytskyi, O.; Blaschke, D. A new class of hybrid EoS with multiple critical endpoints for simulations of supernovae, neutron stars and their mergers. *Eur. Phys. J. A* **2022**, *58*, 152. [CrossRef]
24. Fischer, T.; Blaschke, D.; Hempel, M.; Klähn, T.; Łastowiecki, R.; Liebendörfer, M.; Martínez-Pinedo, G.; Pagliara, G.; Sagert, I.; Sandin, F.; et al. Core collapse supernovae in the QCD phase diagram. *Phys. Atom. Nucl.* **2012**, *75*, 613–620. [CrossRef]
25. Typel, S.; Röpke, G.; Klähn, T.; Blaschke, D.; Wolter, H.H. Composition and thermodynamics of nuclear matter with light clusters. *Phys. Rev.* **2010**, *C81*, 015803. [CrossRef]
26. Baym, G.; Pethick, C.; Sutherland, P. The Ground state of matter at high densities: Equation of state and stellar models. *Astrophys. J.* **1971**, *170*, 299–317. [CrossRef]

27. Glendenning, N.K. First order phase transitions with more than one conserved charge: Consequences for neutron stars. *Phys. Rev. D* **1992**, *46*, 1274–1287. [CrossRef]
28. Verbunt, F.; Phinney, E.S. Tidal circularization and the eccentricity of binaries containing giant stars. *Astron. Astrophys.* **1995**, *296*, 709.
29. Phinney, E.S. Pulsars as Probes of Newtonian Dynamical Systems. *Philos. Trans. R. Soc. Lond. Ser. A* **1992**, *341*, 39–75. [CrossRef]
30. Jiang, L.; Li, X.D.; Dey, J.; Dey, M. A Strange Star Scenario for the Formation of Eccentric Millisecond Pulsar/Helium White Dwarf Binaries. *Astrophys. J.* **2015**, *807*, 41. [CrossRef]
31. Tauris, T.M.; van den Heuvel, P.J. Physics of Binary Star Evolution—From Stars to X-ray Binaries and Gravitational Wave Sources. *arXiv* **2023**, arXiv:2305.09388. [CrossRef]
32. Chanlaridis, S.; Ohse, D.; Aspradakis, N.; Antoniadis, J.; Blaschke, D.; Alvarez-Castillo, D.E.; Danchev, V.; Langer, N. Isolated and eccentric millisecond pulsars from strong phase transitions in neutron star binaries. 2024, *in preparation*.
33. Schaeffer, R.; Zdunik, J.L.; Haensel, P. Phase transitions in stellar cores. I—Equilibrium configurations. *Astron. Astrophys.* **1983**, *126*, 121–145.
34. Lindblom, L. Phase transitions and the mass radius curves of relativistic stars. *Phys. Rev. D* **1998**, *58*, 024008. [CrossRef]